Non-stoichiometry in (001) low temperature GaAs by Raman spectroscopy

2000 J. Phys.: Condens. Matter 12 2895

(http://iopscience.iop.org/0953-8984/12/13/301)

J. Phys.: Condens. Matter **12** (2000) 2895–2902. Printed in the UK PII: S0953-8984(00)07633-5

Non-stoichiometry in (001) low temperature GaAs by Raman spectroscopy

P Puech†, M Toufella†, R Carles†, R Sirvin†, E Bedel‡, C Fontaine‡, M Stellmacher§, R Bisaro§, J Nagle§, A Claverie‖ and G Benassayag‖

† LPST-VMR 5477 CNRS, Université Paul Sabatier, 118 route de Narbonne, 31062 Toulouse Cédex 4, France
‡ LAAS/CNRS, 7 avenue du colonel Roche, 31077 Toulouse Cédex 4, France
§ Thomson-CSF-LCR, domaine de Corbeville, 91404 Orsay Cédex, France
‖ CEMES/CNRS, 29 rue Jeanne Marvig, 31055 Toulouse Cédex 4, France

Received 8 September 1999, in final form 17 January 2000

Abstract. Using the optical phonons as an internal probe, the change in the dielectric permittivity has been analysed by Raman scattering in GaAs grown by MBE at low temperature (LT-GaAs). The screening effect is discussed in terms of a solid solution whereas the strain one is treated in the perfect adhesion hypothesis. Experimentally, the strain and the screening effects have been discriminated by using various scattering geometries. As the LT-layers with large non-stoichiometry have a poor thermal conductivity, it is shown that local heating considerably affects the experimental data. This can be avoided by surface convective exchange then leading to perfect agreement between the recorded phonon frequency shift and the expected ones. As a consequence, this sustains a new method for a quantitative determination of the As excess in LT-layers.

1. Introduction

GaAs grown at low temperature (LT-GaAs) is interesting for both fundamental and applied physics and has been extensively studied over recent years. The carrier lifetimes, as short as 100 fs, are already used in ultra-fast photo-detectors and terahertz sources [1]. In addition, the insulating properties are exploited in electronic structures such as MESFETs and lasers [2]. Before annealing, the LT-GaAs layer is strained onto its substrate. This strain is generally measured by x-ray diffraction, whereas the excess of As is obtained from infra-red spectrometry. During subsequent annealing, the As atoms in excess aggregate into clusters and a semi-insulating behaviour of the layer is observed. Transmission electron microscopy and Raman scattering have been used to determine the mean size of these clusters [3].

Raman spectroscopy has been already applied on LT-GaAs layers. Berg *et al* [4] have observed modes associated to As in GaAs. Then, Gant *et al* [5] interpreted the shift of the GaAs LO phonon as due to the excess of As in terms of (1) reduction of the ionicity and (2) isotropic strain. After that, Calamiotou *et al* [6] used the x-ray data to treat completely the strain field effect on the frequency shift. From the remaining shift and using the virtual crystal approximation, they have deduced an As excess of 3%. This value was not in good agreement with that deduced from their x-ray data (2%).

Very recently, Jackson *et al* [7] have shown that the thermal conductivity is drastically reduced in LT layers. This gives a new insight into the discrepancies observed in previous

0953-8984/00/132895+08$30.00

Raman experimental data. Using conventional experimental procedures may lead to spurious heating effects of the sample.

This work is devoted to Raman measurements on as-grown (001) LT-GaAs layers using specific scattering geometries and good thermalization of the illuminated sample zone. The aim of this paper is to show how the phonon characteristics can thus be used to determine the As excess. Samples and experimental procedure are presented in section 2, and theoretical aspects in section 3. Then, section 4 deals with experimental results. A large part of the discussion is devoted to local heating effects.

2. Samples and experimental aspects

An LT-GaAs sample was grown by molecular beam epitaxy on a semi-insulating (001) GaAs wafer. Its structure is composed of three layers; the first one is 0.8 μm thick and grown at 310 °C, the second is 0.6 μm thick and grown at 280 °C and the top layer is 0.6 μm thick and grown at 240 °C (figure 1). The strain along the growth axis in the different layers was measured by high resolution x-ray diffraction (HRXRD). It has been found to be 4.5, 7.5 and 11.5×10^{-4} respectively. Another sample with only one thick (001) LT-GaAs layer has been grown at 200 °C in order to quantify the heating effects which are shown to greatly modify the Raman response.

Only the LO mode is allowed in the back-scattering configuration on the (001) oriented surface. Moreover, due to the high value of the absorption coefficient in the energy excitation range, the Raman signal originates in the top layer. To obtain information on TO modes, the samples have been cleaved and Raman measurements performed on the high quality (011) oriented cleaved surface. On this surface, only TO modes are allowed.

The Raman data have been recorded at room temperature in the back-scattering geometry using a Dilor micro-probe. Each spectrum has been cleaned from a single CCD burst, and

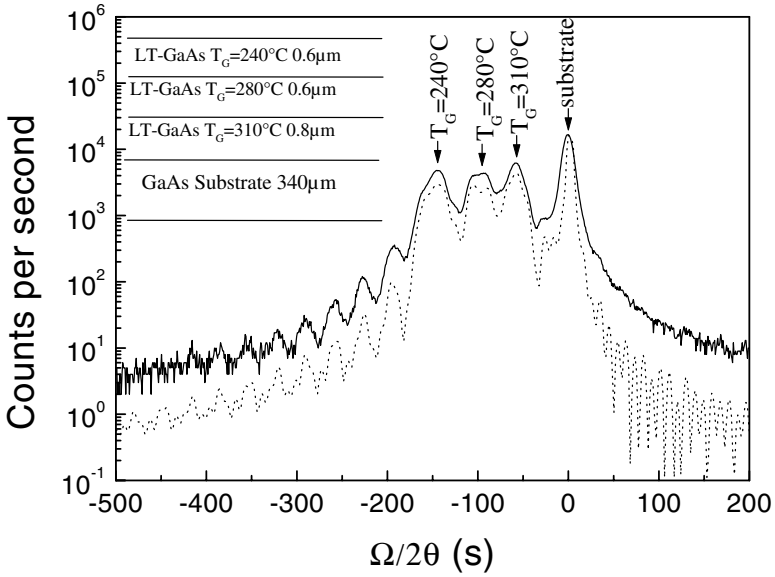

Figure 1. Experimental (continuous line) and simulated (dashed line) curves corresponding to high resolution x-ray diffraction along the (004) plane. The structure of the sample is shown in the inset.

fitted (least squares with relaxation method) using one Lorenztian profile superimposed on a monotonic background. We estimate that the uncertainty in the frequency of the GaAs mode recorded on the layers of interest is about 0.1 cm^{-1}.

In the first part of this paper, we have used the sample with a growth temperature always higher than 240 °C. The spot size was about 1 μm^2 and the laser output power was reduced to 5 mW (i.e. ∼1 mW on the sample) to minimize the heating effects. We have verified that the shift obtained on the top layer is not affected by heating effects. The various LT-layers have been characterized through their respective TO signals.

In the last part of the paper, we have used the sample grown at 200 °C in order to have the worst thermal conductivity and the largest As excess. In order to prevent any heating effect, the spectra have been recorded with the following experimental conditions: a wavelength (647 nm) to decrease absorption (analysed depth of 0.3 μm instead of 0.08 μm for the 488 nm wavelength), a low output power of the laser (10 mW giving 2 mW on the sample), an objective of ×40, and a large flow of cold exchange N_2 gas.

The two bases used are $x||[100]$, $y||[010]$, $z||[001]$ and $X||[110]$, $Y||[1\bar{1}0]$, $Z||[001]$. Using the Porto notation for a given experimental geometry, $\vec{k}_i(\vec{e}_i\vec{e}_s)\vec{k}_s$, where $\vec{k}$ is the photon wavevector and $\vec{e}$ its polarization (i for incident and s for scattered), the corresponding Raman selection rules are reported in table 1.

3. Theory

3.1. Frequency shift due to strain

The As atoms in excess in the GaAs matrix lead to an isotropic strain relative to stoichiometric GaAs, increasing its lattice parameter from a_0 to $a_0(1+\varepsilon)$ for the LT-material. Assuming perfect adhesion of the layer onto the substrate, the layer in-plane lattice parameter is reduced to the bulk value of GaAs, whereas its lattice parameter along the growth axis, $a_\perp$, is extended. The in-plane and out of plane strain may be expressed as

$$\varepsilon_\parallel = 0 \qquad \text{and} \qquad \varepsilon_\perp = \frac{a_\perp - a_0}{a_0} = \varepsilon - \frac{2S_{12}}{S_{11}+S_{12}}\varepsilon = \frac{S_{11}-S_{12}}{S_{11}+S_{12}}\varepsilon \tag{1}$$

where S_{ij} are the contracted components of the fourth-rank compliance tensor.

The frequency shifts, $\Delta\omega$, of TO or LO modes (S stands for singlet and D for doublet) are given by the following:

$$\Delta\omega_S = \frac{\omega_0}{2}\tilde{K}_{11}\varepsilon_\perp \tag{2}$$

$$\Delta\omega_D = \frac{\omega_0}{2}\tilde{K}_{12}\varepsilon_\perp \tag{3}$$

where ω_0 is the bulk frequency and $\tilde{K}_{ij}$ are the phonon deformation potentials. Different scattering geometries have to be used to determine these phonon deformation potentials [5] and in our case to evaluate strain effects.

3.2. Frequency shift due to screening

The TO and LO frequencies can be derived from the dielectric function

$$\varepsilon(\omega) = \varepsilon_\infty + \frac{Ne^2}{\mu(\omega_{TO}^2 - \omega^2 + \mathrm{i}\Gamma\omega)} = \varepsilon_\infty\left\{1 + \frac{\omega_{LO}^2 - \omega_{TO}^2}{(\omega_{TO}^2 - \omega^2 + \mathrm{i}\Gamma\omega)}\right\} \tag{4}$$

where N is the density of Ga–As oscillators, μ their reduced mass, e their effective charge and Γ their damping frequency. The LO frequency is the pole of $\mathrm{Im}\{-1/\varepsilon\}$ and the TO the pole of ε. The ionic plasmon frequency, ω_p is then defined as follows:

$$\omega_{LO}^2 = \omega_{TO}^2 + \omega_p^2 \qquad \text{with } \omega_p^2 = \frac{Ne^2}{\mu\varepsilon_\infty}. \tag{5}$$

To evaluate the variation of this ionic plasmon frequency, one can introduce a reference frequency ω_c, defined by

$$\frac{\Delta\omega_p^2}{\omega_p^2} = \frac{\Delta\omega_{LO}}{\omega_c} \qquad \text{with } \omega_c = \frac{\omega_p^2}{2\omega_{LO}}. \tag{6}$$

It is interesting to note that only the LO mode is related to the ionic plasmon frequency and is sensitive to the screening effect. This will be exploited to evaluate this effect.

3.3. Application to LT-GaAs

The LO and TO frequencies in bulk GaAs at 300 K are $\omega_{LO} = 292.6\ \mathrm{cm}^{-1}$ and $\omega_{TO} = 269.3\ \mathrm{cm}^{-1}$ respectively [8], leading to $\omega_c = 22.4\ \mathrm{cm}^{-1}$. The strain induced shifts have been calculated (table 1) using the experimental values of their deformation potentials [9] and equations (2) and (3):

$$\tilde{K}_{11}(\mathrm{LO}) = -1.71 \qquad \tilde{K}_{12}(\mathrm{LO}) = -2.42$$
$$\tilde{K}_{11}(\mathrm{TO}) = -2.38 \qquad \tilde{K}_{12}(\mathrm{TO}) = -2.68.$$

Using the compliance component values for GaAs [10] and equation (1), $\varepsilon_\perp$ has been found to be equal to 1.902ε.

Like many authors, we roughly identify [10] the excess of antisite related defect to the excess of arsenic, $x = ([\mathrm{As}]-[\mathrm{Ga}])/([\mathrm{As}]+[\mathrm{Ga}])$. The lattice parameter variation in LT-GaAs has been experimentally related to this excess through [11]

$$\varepsilon_\perp = 0.068x. \tag{7}$$

To estimate the screening effect in LT-GaAs, Gant *et al* [5] proposed to use a virtual crystal approximation to analyse the LO frequency shift as resulting from a 'one-mode behaviour'. This implies that the As–As and Ga–As frequencies are very close. The As–As optical frequencies are however known to be much lower than Ga–As, and this should prevent any coupling.

In our opinion, an approach in terms of a two-mode behaviour should be therefore more appropriate [12]. For small x values, the LT material should then behave as a solid solution, $(\mathrm{GaAs})_{1-x}(\mathrm{AsAs})_x$, whose dielectric function is:

$$\varepsilon(\omega, x) = \varepsilon_\infty(x)\left\{1 + \frac{\omega_p^2(x)}{(\omega_{TO}^2 - \omega^2 + \mathrm{i}\Gamma\omega)}\right\} \tag{8}$$

with

$$\omega_p^2(x) = (1-x)\frac{\varepsilon_{\infty,GaAs}}{\varepsilon_\infty(x)}\omega_p^2 \qquad \text{and} \qquad \varepsilon_\infty(x) = (1-x)\varepsilon_{\infty,GaAs} + x\varepsilon_{\infty,GaAs}. \tag{9}$$

In these equations, the effective charge associated with the covalent As–As bonds has been taken as zero, and the $\varepsilon_{\infty,Ge}$ value can be used for $\varepsilon_{\infty,As}$ according to previous experimental work [13] and theoretical considerations [14]. In order to calculate the frequency shift due to screening ($\Delta\omega$), the change in the number (N) of Ga–As oscillators (see equation (9)) and the effect of their electronic screening (s) on ε_∞ (see equation (8)) have to be taken into account. They contribute as $-22.4x$ and $-7.7x$ respectively, leading to

$$\Delta\omega(\mathrm{cm}^{-1}) = -30.1x. \tag{10}$$

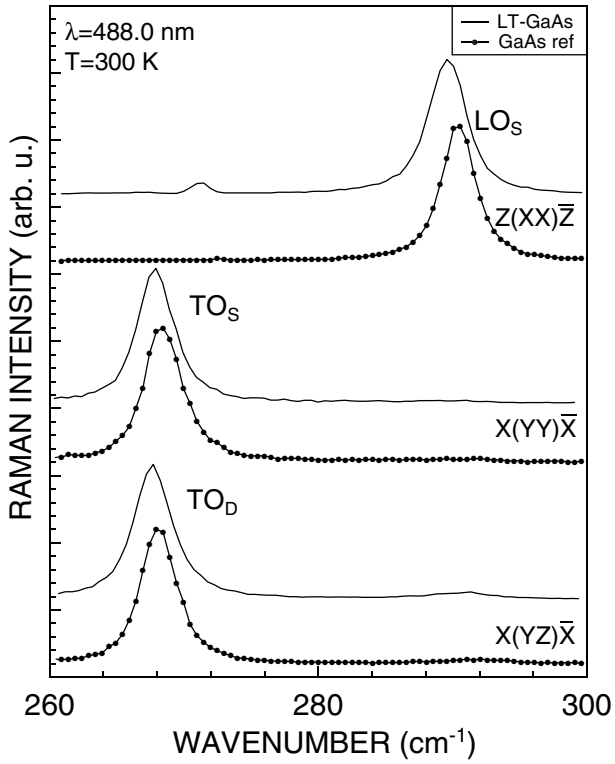

Figure 2. Raman selection rules obtained from the top layer of the structure.

Table 1. Raman selection rules and phonon frequency shift for different experimental configurations. In columns 5 and 6 are reported the phonon frequency shift deduced from Raman measurement and calculated using HRXRD data. The remaining shift is attributed to screening effects in the dielectric permittivity $\varepsilon(\omega)$.

Configuration	Activated Raman tensor	Phonon component	$\Delta\omega/\varepsilon_\perp$ (cm^{-1})	$\Delta\omega$ (cm^{-1}) Raman	$\Delta\omega$ (cm^{-1}) from x-ray	$\Delta\omega$ (cm^{-1}) due to $\varepsilon(\omega)$
$Z(XX)\bar{Z}$	$\Gamma_{15}(Z)$	LO$_S$	−251	-0.4 ± 0.2	−0.37	—
$X(YZ)\bar{X}$	$\Gamma_{15}(Y)$	TO$_D$	−351	-0.4 ± 0.2	−0.41	—
$X(YY)\bar{X}$	$\Gamma_{15}(Z)$	TO$_S$	−321	-0.82 ± 0.1	−0.28	−0.54
$x(yz)\bar{x}$	$\Gamma_{15}(x)$	LO$_D$	−351	—	−0.4	—

4. Experimental results

Typical Raman spectra are reported in figure 2. The expected Raman selection rules are observed to be well verified in LT layers as in bulk GaAs. Moreover the full width at half maximum and shape of the phonon lines are similar in both materials. These results indicate that the crystalline quality of the GaAs matrix in LT layers is good and consequently that disorder effects can be neglected [15]. A small downshift of the TO and LO GaAs phonon frequencies is observed. This cannot be exclusively accounted for by the effect of strain (see table 1), as the LO shift is more than twice the TO one. This reveals that screening effects have also to be taken into account.

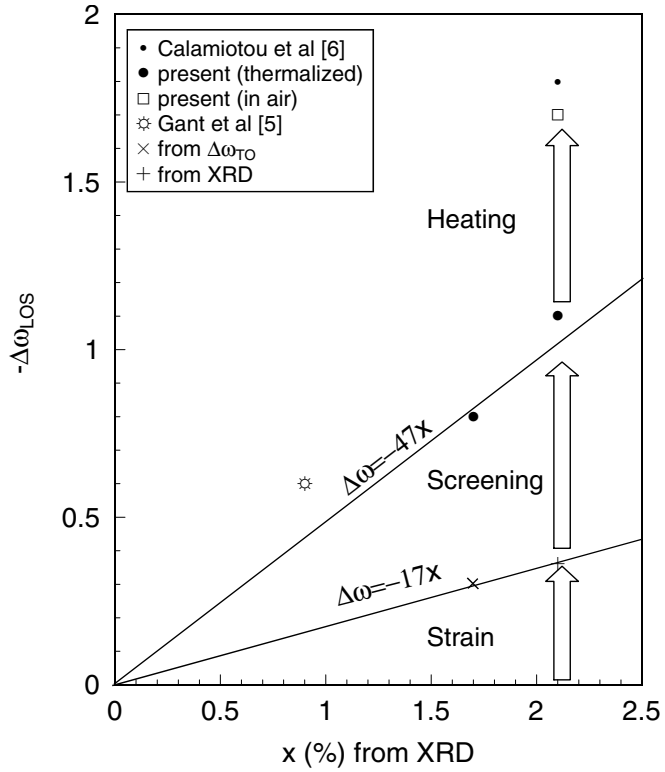

Figure 3. Absolute frequency shift of the LO mode versus the As excess deduced from x-ray data.

4.1. Strain effects

The strain in the top layer was evaluated from the TO mode, as this is only sensitive to strain. The TO frequency shifts for both the singlet and doublet TO modes are reported in table 1. Using strain values derived from HRXRD measurements, the TO phonon frequency shifts have been calculated using table 1. Within the experimental uncertainties a quite good agreement between experimental and calculated values is observed.

4.2. Screening effects and quantitative determination of As excess

The screening effect has been evaluated through analysis of the LO mode. This mode can be analysed in back-scattering geometry from the surface. Because strain and screening effects can both account for the LO downshift, the frequency shift due to strain has been calculated first. Its value has been found to be equal to $-0.28\ \mathrm{cm}^{-1}$, using equation (2) ($\Delta\omega_{strain} = -17x$). It has been then subtracted from the total shift (table 1). The remaining part is attributed to the screening effect.

This shift is related to the As excess present in the LT-layer by $\Delta\omega\,(\mathrm{cm}^{-1}) \approx -30x$. This fits the theoretical estimation (see equation (10)).

4.3. Heating effects

The expression $\Delta\omega\,(\mathrm{cm}^{-1}) \approx -30x$ does not fit the other published data as shown in figure 3 where $-\Delta\omega_{LOS}$ is reported as a function of the x excess. We will show that these discrepancies

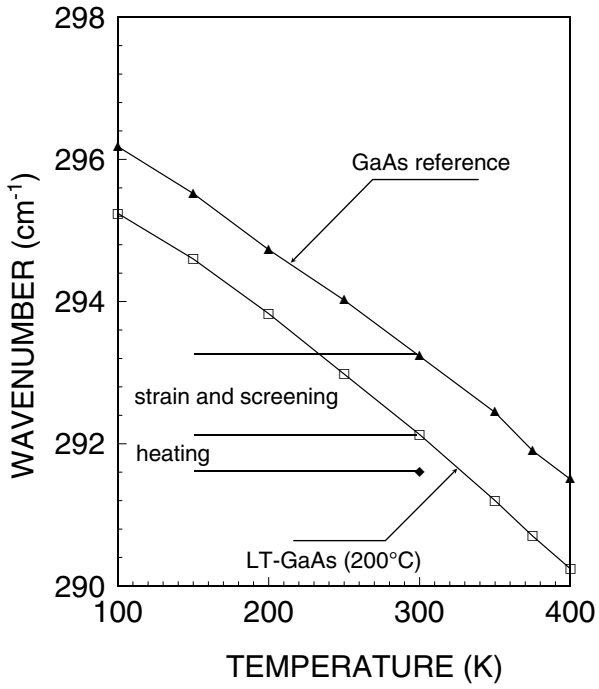

Figure 4. Variation of the frequency shift versus temperature when subjecting the surface to an N_2 flux. The squares correspond to measurements performed in air.

can be accounted for by taking into account drastic heating effects in these low thermal conductivity materials [7].

In amorphous GaAs, such effects are also present, leading to a typical temperature increase of 30 °C in air and 40 °C in vacuum [16]. In the case of small particles, the degradation of the thermal conductivity leads to black body emission [17]. The thermalized sample holder can not play its role perfectly, as it is separated from the heated volume by a layer with an high thermal resistivity.

For the sample grown at 200 °C and with the experimental conditions detailed in section 2, we have obtained a frequency shift of -1.7 cm^{-1} when the measurements are performed in air, i.e. without convective exchange of heat. This shift is similar to those obtained by Calamiotou *et al* [6] with a sample grown at the same temperature. Conversely, this shift is decreased to -1.1 cm^{-1} when the surface has been exposed to a stream of cold N_2 gas. As shown in figure 4, this shift is observed to remain constant with temperature. Moreover, the variation of LO GaAs frequency follows the same behaviour with temperature as the one previously obtained with an Oxford CF204 continuous helium flow cryostat [8]. It is worth noting that the frequency shift measured in the LT-GaAs layers is constant with temperature. This shows the absence of any electronic coupling effect.

Our results provide evidence that the Raman analysis can be highly affected by sample heating, which is related to the poor thermal conductivity of LT-materials and that care must then be taken into in order to prevent this spurious effect.

The frequency shift of the LO mode measured for an LT-layer is then equal to $-17x$ for its strain component and $-30x$ for its screening component. One can take advantage of this simple experimental compositional dependence to easily determine by Raman spectroscopy

the As excess in an LT-GaAs layer (x) from the frequency shift of the GaAs LO mode ($\Delta\omega_{LOS}$), as $x = -\Delta\omega_{LOS}/47$.

5. Conclusion

Detailed analysis of frequency shifts of the matrix optical phonons in LT-GaAs layers has shown that two main effects have to be considered: (i) the strain due to the As excess and the resulting mismatch with the substrate, and (ii) the electronic screening of the ionic plasmon frequency. This analysis is based on the different behaviour of the TO and polar LO modes, whose signals have been recorded using specific experimental configuration geometries. The capability of the Raman technique, when using appropriate experimental conditions, to obtain information on the strain and the excess of As in LT-layers has been demonstrated.

Acknowledgment

This work was financially supported by a research programme of the Région de Midi-Pyrénées.

References

[1] Lai R K, Hwang J R, Norris T B and Whitaker J F 1998 *Appl. Phys. Lett.* **24** 3100–3
[2] Sin Y K and Horikawa H 1995 *Japan. J. Appl. Phys.* **34** L125–6
[3] Toufella M, Puech P, Carles R, Bedel E, Fontaine C, Claverie A and Benassayag G 1999 *J. Appl. Phys.* **85** 2929–39
[4] Berg R S, Mavalvala N, Steinberg T and Smith F W 1990 *J. Electron. Mater.* **19** 1323
[5] Gant T A, Shen H, Flemish J R, Fotiadis L and Dutta M 1992 *Appl. Phys. Lett.* **60** 1453–6
[6] Calamiotou M, Raptis Y S, Anastassakis E, Lagadas M and Hatzopoulos Z 1993 *Solid State Commun.* **87** 563
[7] Jackson A W, Ibbetson J P, Gossard A C and Mishra U K 1999 *Appl. Phys. Lett.* **74** 2325
[8] Puech P, Landa G, Carles R and Fontaine C 1997 *J. Appl. Phys.* **82** 4493
[9] Wickboldt P, Anastassakis E, Sauer R and Cardona M 1987 *Phys. Rev.* B **35** 1362
[10] *Landolt–Börnstein New Series* 1982 vol 17a (New York: Springer) p 235
[11] Liu X, Prasad A, Nishio J, Weber E R, Liliantal-Weber Z and Walukiewicz W 1995 *Appl. Phys. Lett.* **67** 279
[12] Groenen J, Carles R, Landa G, Guerret-Piecourt C, Fontaine C and Gendry M 1998 *Phys. Rev.* B **58** 10 452
[13] Burns G, Dacol F H, Wie C R, Burstein E and Cardona M 1987 *Solid State Commun.* **62** 449–54
[14] Harrison W A and Pantelides S T 1976 *Phys. Rev.* B **14** 691
[15] Maury F, Carles R, Landa G and Renucci J B 1987 *Thin Solid Films* **155** 331
[16] Chehaidar A, Zwick A, Carles R and Bandet J 1994 *Phys. Rev.* B **50** 5345
[17] Roura P, Costa J, Lopez-de Miguel M, Garrido B, Fort J, Morante J R and Bertran E 1999 *J. Lumin.* **80** 518